Acta Crystallographica Section D
Biological Crystallography
ISSN 0907-4449

Structure of the biotin carboxylase domain of pyruvate carboxylase from *Bacillus thermodenitrificans*

Shin Kondo,[a,b] Yoshitaka Nakajima,[b] Shigetoshi Sugio,[a,b]* Shinji Sueda,[c] Md Nurul Islam[c] and Hiroki Kondo[c]*

[a]ZOEGENE Corporation, Aoba, Yokohama 227-8502, Japan, [b]Science and Technology Office, Mitsubishi Chemical Corporation, Aoba, Yokohama 227-8502, Japan, and [c]Department of Biochemical Engineering and Science, Kyushu Institute of Technology, Iizuka 820-8502, Japan

Correspondence e-mail: 4204153@cc.m-kagaku.co.jp, kondo@bio.kyutech.ac.jp

Received 5 March 2007
Accepted 15 June 2007

PDB Reference: biotin carboxylase domain of pyruvate carboxylase, 2dzd, r2dzdsf.

The biotin carboxylase (BC) domain of pyruvate carboxylase (PC) from *Bacillus thermodenitrificans* (BC-bPC) was crystallized in an orthorhombic form (space group $P2_12_12_1$), with unit-cell parameters a = 79.6, b = 116.0, c = 115.7 Å. Two BC protomers are contained in the asymmetric unit. Diffraction data were collected at 100 K and the crystal structure was solved by the molecular-replacement method and refined against reflections in the 20.0–2.4 Å resolution range, giving an R factor of 0.235 and a free R factor of 0.292. The overall structure of BC-bPC is similar to those of the BC subunits of *Aquifex aeolicus* PC (BC-aPC) and *Escherichia coli* ACC (BC-eACC). The crystal structure revealed that BC-bPC forms a unique dimeric quaternary structure, which might be caused as a result of the division of the BC domain from the rest of the protein. The position of domain *B* in BC-bPC differs from those in other enzymes of similar structure (BC-aPC and BC-eACC).

1. Introduction

Pyruvate carboxylase (PC; EC 6.4.1.1) is located at the junction of glycolysis and the citric acid cycle and participates in gluconeogenesis by mediating the carboxylation of pyruvate to oxalacetate (Jitrapakdee & Wallace, 1999; Scrutton, 1978). PC is distributed in eukaryotes as well as in some prokaryotes and is composed of three functional domains named biotin carboxylase (BC), carboxyl transferase (CT) and biotin carboxyl carrier protein. These domains either reside on a single polypeptide chain of 130 kDa or constitute two subunits of 70 and 50 kDa (Wood & Barden, 1977). The former type of PC is distributed in eukaryotes and some prokaryotes, while the latter is found only in prokaryotes such as *Pseudomonas citronellolis* (Taylor *et al.*, 1972). The reaction of PC and of other biotin-dependent carboxylases such as acetyl-CoA carboxylase (ACC) and propionyl-CoA carboxylase proceeds in two steps. Enzyme-bound biotin is first carboxylated by bicarbonate and ATP and the carboxyl group bound temporarily on biotin is subsequently transferred to an acceptor substrate such as pyruvate and acetyl-CoA (Wood & Barden, 1977; Attwood, 1995). The first reaction is mediated by the BC domain or subunit and is common to all biotin-dependent carboxylases, whereas the second reaction mediated by the CT domain or subunit differs from enzyme to enzyme depending on the substrate to be carboxylated (Wood & Barden, 1977).

One characteristic feature of single polypeptide chain-type PCs is that their reaction is subject to allosteric regulation by acetyl-CoA and aspartate, which activate and deactivate the enzyme, respectively (Jitrapakdee & Wallace, 1999; Cazzulo &

Table 1
Data-collection statistics for BC-bPC.

Values in parentheses are for the outermost shell (2.49–2.40 Å resolution).

Resolution range (Å)	20–2.4
No. of measured reflections	300188
No. of unique reflections	42671
Completeness (%)	99.9 (99.4)
Average $I/\sigma(I)$	30.3 (7.8)
R_{sym}† (%)	8.8 (28.8)
Cell lattice	Orthorhombic
Space group	$P2_12_12_1$
Unit-cell parameters (Å)	
a	79.6
b	116.0
c	115.7

† $R_{sym} = \sum |I - \langle I \rangle| / \sum I \times 100$.

Table 2
Structure-refinement statistics for BC-bPC.

Values in parentheses are for the outermost shell (2.42–2.40 Å resolution).

Resolution range (Å)	20–2.4
$R_{working}$†	0.235 (0.263)
R_{free}‡	0.292 (0.302)
No. of reflections used	42429
No. of protein atoms	7175
No. of solvent atoms	349
Average *B* factor (Å^2)	
All atoms	25.2
Protein atoms	25.2
Solvent atoms	25.4
Root-mean-square deviations from ideality	
Bond lengths (Å)	0.006
Bond angles (°)	1.2
Torsion angles (°)	23.2

† $R_{working}$ is calculated from 95% of reflections used for refinement [$R_{working} = (\sum |F_{obs} - F_{calc}| / \sum |F_{obs}|)$]. ‡ R_{free} is calculated from 5% of reflections excluded from refinement.

Stoppani, 1968; Attwood, 1993), whereas subunit-type PCs are independent of allosteric regulation (Cohen *et al.*, 1979; Mukhopadhyay *et al.*, 1998). Three-dimensional structures of the BC subunit of *Escherichia coli* ACC (abbreviated BC-eACC) both alone and in complex with ATP have been reported previously (Waldrop *et al.*, 1994; Thoden *et al.*, 2000). The structure of the BC subunit of acetyl-CoA-independent PC from *Aquifex aeolicus* (abbreviated BC-aPC) has also recently been reported (Kondo *et al.*, 2004). There are ample data to suggest that the BC rather than the CT reaction is subject to allosteric regulation (Attwood, 1995; Sueda *et al.*, 2004). This in turn implies that the BC domain possesses an acetyl-CoA-binding site and this notion prompted us to study the structure of the BC domain of an acetyl-CoA-dependent PC. Here, we report the structure of the BC domain of such a PC from *Bacillus thermodenitrificans* (abbreviated BC-bPC), with the aim of hopefully gaining insight into the origin of allosterism in PC.

2. Materials and methods

2.1. Expression and purification

The divided BC domain of *B. thermodenitrificans* PC (BC-bPC, 461 residues) was prepared as described previously (Sueda *et al.*, 2004). Its amino-acid sequence is 48% identical to that of BC-aPC over 457 residues.

2.2. Crystallization and data collection

Crystallization of BC-bPC was carried out at 293 K by the hanging-drop vapour-diffusion method. A 5.0 µl droplet of protein solution (10.0 mg ml^{-1} protein solution mixed with the same amount of reservoir solution) was equilibrated against 100 µl reservoir solution containing 2%(*w*/*v*) PEG 8000, 100 m*M* Tris–HCl buffer pH 7.8. Needle-shaped crystals grew to dimensions of 0.005 × 0.005 × 0.5 mm in a few days and diffracted to 3.0 Å resolution. To obtain a higher resolution data set, the crystallization condition was optimized by adding 0.75 µl of a 1.0%(*w*/*v*) agarose solution to 5.0 µl of the mother-liquor droplet. Needle-shaped crystals grew to dimensions of 0.03 × 0.03 × 0.5 mm in a week and belonged to space group $P2_12_12_1$, with unit-cell parameters *a* = 79.6, *b* = 116.0, *c* = 115.7 Å. Assuming the presence of two molecules in the asymmetric unit, the Matthews coefficient V_M was calculated to be 2.60 Å^3 Da^{-1}, indicating a solvent content of approximately 53% in the unit cell. These values are within the range typical for protein crystals (Matthews, 1968). For data collections under cryogenic conditions, crystals were soaked for a few seconds in a solution containing 15%(*v*/*v*) PEG 400, 10%(*v*/*v*) 2-methyl-2,4-pentanediol, 15%(*w*/*v*) PEG 8000 and 100 m*M* Tris–HCl buffer pH 7.8. Crystals were mounted in a nylon loop and flash-cooled in a liquid-nitrogen stream at 100 K. Data collection was performed at 100 K with a Rigaku Jupiter CCD detector system using a monochromated X-ray beam (wavelength 0.836 Å) at the BL24XU station of SPring-8 (Hyogo, Japan). Diffraction data were processed using *HKL*-2000 (Otwinowski & Minor, 1997), giving a completeness of 100.0% in the resolution range 20.0–2.40 Å with an R_{sym} of 8.8% (Table 1).

2.3. Structure determination and refinement

A set of initial phases was obtained by molecular replacement using the structure of the BC subunit of *A. aeolicus* PC (BC-aPC; PDB code 1ulz) as a search model. Two solutions with the highest correlation coefficients were obtained from a calculation using the program *EPMR* (Kissinger *et al.*, 1999). The model of one molecule was built into electron density calculated from the initial phases using *XtalView* (McRee, 1993), while that of the other subunit in the asymmetric unit was generated using local twofold symmetry. The structure of BC-bPC was first refined by simulated annealing and energy minimization with the program *CNX* (Brünger *et al.*, 1998) using X-ray data from 20 to 2.4 Å resolution. However, the *R* factor and R_{free} did not reduce below 31.5% and 40.8%, respectively. As the residues Ile136–Ile208 in both molecules were not clearly visible in the calculated map, the model was rebuilt using a $2F_o - F_c$ OMIT map. Water molecules with a temperature factor above 50 Å^2 after refinement were excluded from the model. Several rounds of refinement and manual rebuilding resulted in an *R* factor of 23.5% and R_{free} of

29.2% using 42 429 reflections between 20 and 2.4 Å resolution (Table 2).

3. Results and discussion

3.1. Quality of the structure

The asymmetric unit of the BC domain of a *B. thermodenitrificans* PC (BC-bPC) crystal accommodates two monomers of BC and these molecules are related by a noncrystallographic twofold axis. The refined model comprised 459 residues for molecule 1 (mol1), 453 residues for molecule 2 (mol2) and 349 water molecules. Other statistics at the final refinement stage are summarized in Table 2. This final model lacks the two N-terminal residues for mol1 and eight residues for mol2, including the six residues Ala195–Asp200 as well as two at the N-terminus, owing to a lack of interpretable electron density. The average temperature factor for the main-chain atoms in mol1 and mol2 were 24.3 and 26.0 Å^2, respectively, with the maximum temperature factors being 45.3 and 73.5 Å^2. Water molecules included in the final model gave an average *B* factor of 25.4 Å^2 and a maximum *B* factor of 49.6 Å^2. Analysis of the stereochemistry using *PROCHECK* (Laskowski *et al.*, 1993) revealed that most of the nonglycine residues fell within the most favoured region (89.6%) or the additional allowed region (9.7%) of the Ramachandran plot (Ramachandran & Sasisekharan, 1968). The root-mean-square deviations of the bond length, angles and torsion angles were in good agreement with ideal values (Table 2).

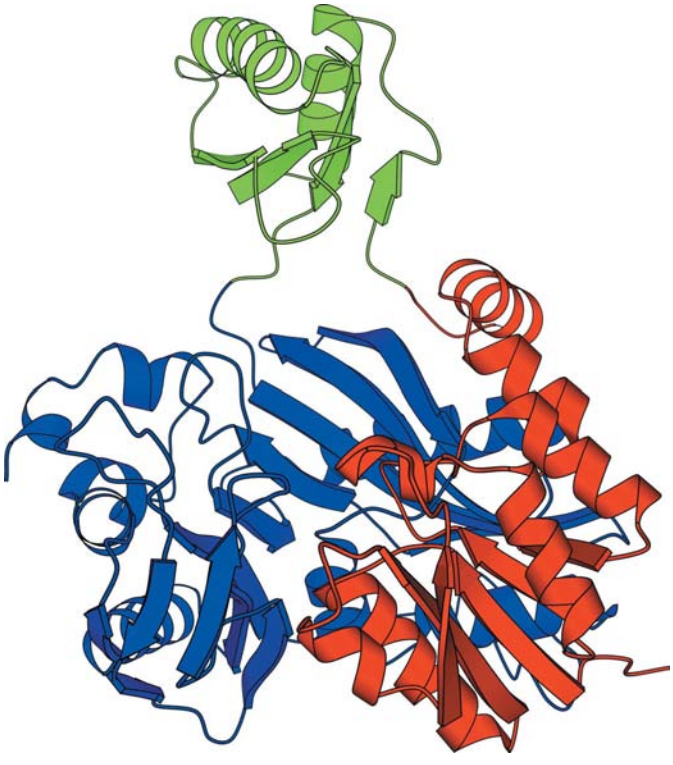

Figure 1
Overall schematic structure of BC-bPC illustrated using the program *MOLSCRIPT* (Kraulis, 1991). Domains *A*, *B* and *C* are shown in red, green and blue, respectively.

3.2. Overall structure

The backbone trace of BC-bPC is shown in Fig. 1. Its overall structure is very similar to those of the BC subunits of *A. aeolicus* PC (BC-aPC) and *E. coli* ACC (BC-eACC). BC-bPC comprises 17 α-helices and 23 β-strands; 35% of the residues are contained in α-helices and 28% in β-strands. The content of these ordered structures is slightly smaller than that of BC-aPC (Kondo *et al.*, 2004), which may be associated with a difference in their thermal stability. BC-bPC consists of three domains, *A* (Thr3–Val135), *B* (Ile136–Glu209) and *C* (Asn210–Phe459), and its molecular architecture is similar to that of BC-aPC (Kondo *et al.*, 2004), BC-eACC (Waldrop *et al.*, 1994) and NAD$^+$-dependent dehydrogenases (Waldrop *et al.*, 1994). The molecular dimensions of domains *A* and *C* are approximately 55 × 55 × 30 Å and those of domain *B* are 22 × 28 × 25 Å.

The N-terminal domain (domain *A*) consists of five β-strands in a parallel β-sheet and four α-helices that flank each side of the β-sheet. Domain *B* has two α-helices, four β-strands and a glycine-loop region (residues Leu166–Gly172) that plays a crucial role in ATP binding (Thoden *et al.*, 2000). The C-terminal domain (domain *C*) consists of eight β-strands, an antiparallel β-sheet of half-barrel form, four other β-strands and eight α-helices. These helices exist at the back of (Ser253–Ser270), inside (Gln300–Gly309) and under the barrel (Asp311–Gly322) and near the C-terminus (Phe407–Glu420, Asn429–Gln438, His439–Ser444, Thr449–Thr454, Pro456–Val460). Of the 17 proline residues in BC-bPC, two, Pro159 and Pro248, assume *cis* conformation; the electron density of these residues was very clearly visible. Since these two proline residues are conserved in BC-aPC and BC-eACC (Kondo *et al.*, 2004; Waldrop *et al.*, 1994), they may be important in forming the molecular structure of BC.

Despite the gross similarity in the overall folding of BC-bPC to that of BC-aPC and BC-eACC, there is a short loop in the

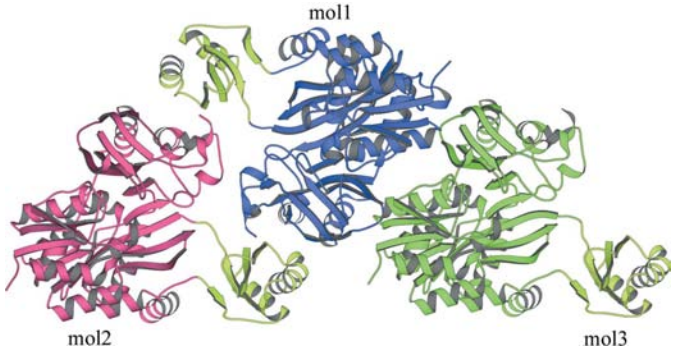

Figure 2
Crystal-packing scheme for BC-bPC. Mol1 (blue) and mol2 (red) are molecules in the asymmetric unit and they are related by a noncrystallographic twofold axis. Mol3 (green) was generated by the simple cell translation of mol2. The structures of domain *B* of each molecule are shown in yellow.

Table 3
Electrostatic interactions observed for BC-bPC.

Mol1–mol2 contacts (see Fig. 2)

Atom name, mol1	Atom name, mol2	Distance (<3.4 Å)	Domains
Gly172 N	Phe461 OXT†	2.928	*B–C*
Gly172 N	Phe461 O	2.624	*B–C*
Arg177 NH1	Gln438 OE1	3.14	*B–C*
Arg177 NH2	Glu457 OE1	2.927	*B–C*
Arg188 NE	Glu434 OE1	3.129	*B–C*
Arg188 NH1	Gln434 OE1	2.984	*B–C*
Arg188 NH1	Gln438 OE1	3.062	*B–C*
Arg188 NH2	Glu434 OE1	3.319	*B–C*
Gln438 OE1	Arg174 NH1	3.152	*C–B*
Glu457 OE2	Arg177 NH2	3.228	*C–B*
Arg412 NH1	Glu184 OE2	3.381	*C–B*
Arg412 NH2	Glu184 OE2	3.095	*C–B*

Mol1–mol3 contacts (see Fig. 2).

Atom name, mol1	Atom name, mol3	Distance (<3.4 Å)	Domains
Glu329 O	Phe374 N	2.578	*C–C*
Gly371 O	Arg4 NH2	2.848	*C–A*
Phe374 N	Glu328 O	3.016	*C–C*
Gln385 OE1	Arg7 NE	3.149	*C–A*
Arg4 NH2	Gly371 O	2.708	*A–C*
Arg31 NH2	Tyr44 OH	3.065	*A–A*
Arg416 NH2	His328 ND1	3.347	*C–C*

† C-terminal O atom.

former inserted between the α-helix consisting of residues 311–322 and the β-strand consisting of residues 342–351. This short insertion sequence (Glu329–Lys334 in BC-bPC) is found in PCs whose activity is modulated by acetyl-CoA, although the inserted sequence is not highly conserved across this class

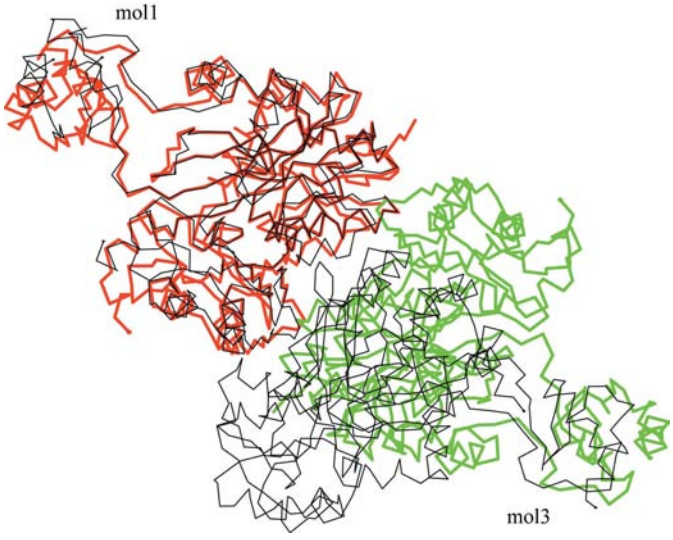

Figure 3
C^{α} models created by superimposing two molecules of BC-bPC and the dimer of BC-eACC (open form; PDB code 1bnc; Waldrop *et al.*, 1994). Mol1 and mol3 in this figure correspond to mol1 and mol3 in Fig. 2, respectively. Structural superposition was made with C^{α} atoms belonging to mol1 and chain *A* of BC-eACC (thick red and black lines, respectively). Mol3 of BC-bPC and chain *B* of BC-eACC are shown in thick green and black lines, respectively.

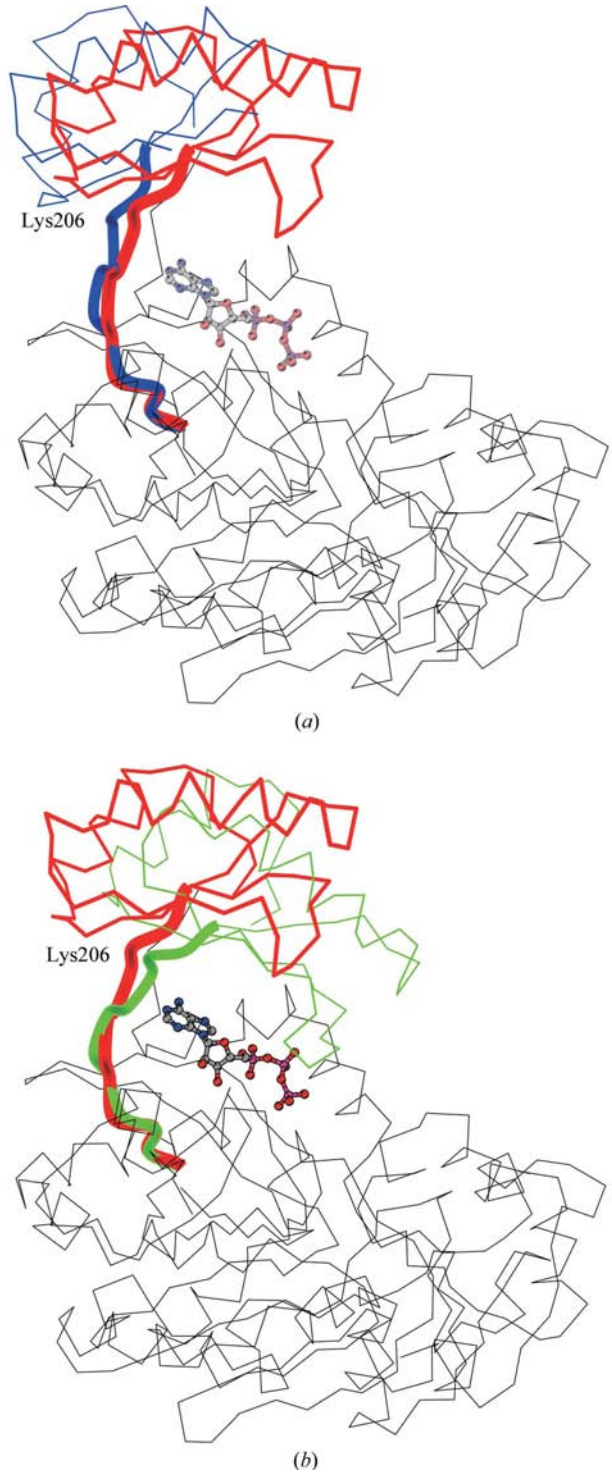

Figure 4
Comparison of the conformation of domain *B* of BC-bPC and BC-eACC with an emphasis on the loop region. (*a*) Superposition of BC-bPC (black lines, domains *A* and *C*; thick red lines, domain *B*) on domain *B* (blue lines) of BC-eACC (unliganded open form). (*b*) The C^{α} model of BC-bPC (black lines, domains *A* and *C*; thick red lines, domain *B*) is superimposed on domain *B* (green lines) of liganded BC-eACC (ATP-bound closed form). The linkers from Val204 to Glu215 of BC-bPC (red lines) and the corresponding sequence of BC-eACC (blue or green lines) are emphasized using thick lines. It is noticed that the loop of BC-bPC is positioned between the open (*a*) and closed forms of BC-eACC (*b*). In the two schemes, the ATP model of liganded ACC is superimposed on the binding site of BC-bPC.

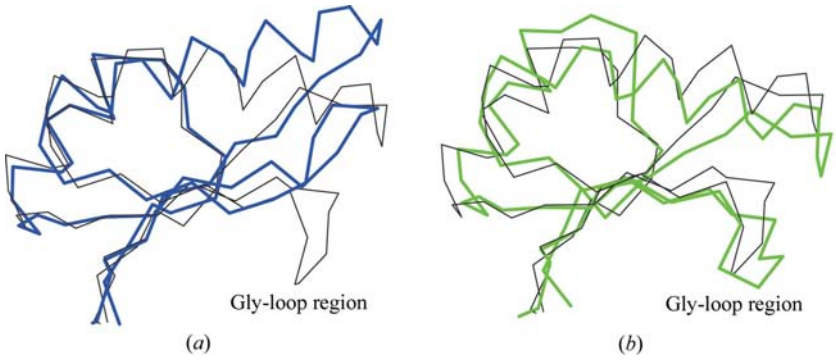

Figure 5
Schemes representing superimposed C^{α} models of BC-bPC and part of domain *B* from other BC subunits. (*a*) Model of superimposed BC-bPC and domain *B* of BC-aPC (open form). (*b*) Model of superimposed BC-bPC and domain *B* of liganded BC-eACC (ATP-bound closed form).

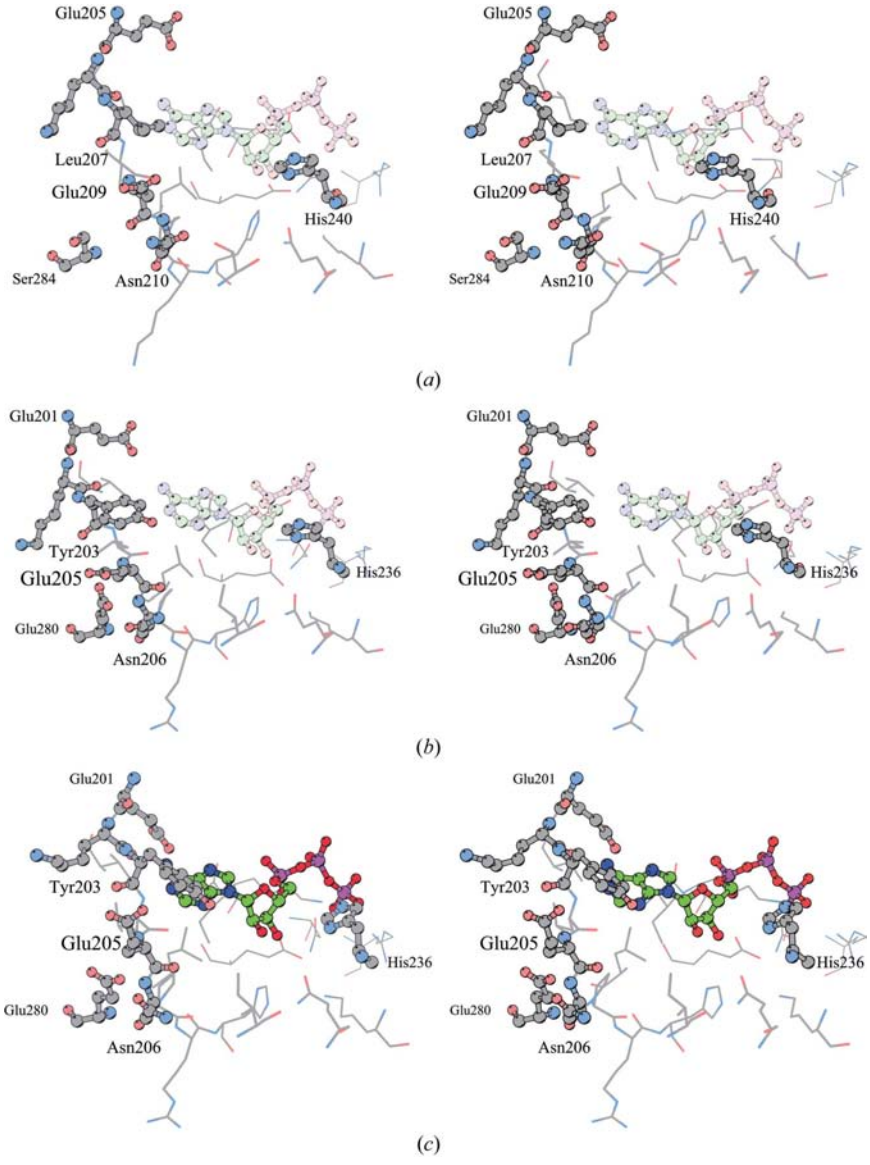

Figure 6
Three types of active-site structure of BC shown as stereoviews. (*a*), (*b*) and (*c*) show BC-bPC, unliganded BC-eACC (ATP-unbound open form) and liganded BC-eACC (ATP-bound closed form), respectively. The ATP models in (*a*) and (*b*) show the ATP model from liganded ACC virtually superimposed on the active site (light-coloured model).

of PCs. Whether this is associated with acetyl-CoA binding is discussed below.

3.3. Quaternary structure and crystal packing

The crystal-packing scheme of BC-bPC is shown in Fig. 2. The asymmetric unit of BC-aPC contains two molecules of the protein which are related by a noncrystallographic twofold axis (mol1–mol2 in Fig. 2). Their association state in the crystal differs from that of BC-aPC (Kondo *et al.*, 2004) and BC-eACC (Waldrop *et al.*, 1994); domain *B* of mol1 and domain *C* of mol2 are adjacent to each other in the former, whereas the sides composed of domains *A* and *C* face each other with domain *B* located away in the latter two proteins. As a result, the substrate-binding sites of each monomer of BC-bPC are located adjacent to each other (Fig. 2). The dimer structure has two types of association: in the first the dimer is related by a noncrystallographic symmetric operation (mol1–mol2 in Fig. 2) and in the second it is contacted by a molecule (mol3) present in the neighbouring unit cell (mol1–mol3 in Fig. 2). The association mode of mol1 and mol3 appears to be similar to that of the dimeric structures of BC-eACC and BC-aPC, but when either one of the dimer molecules is overlaid the location of the other molecule definitely differs between the two structures (Fig. 3). Thus, C^{α} of Glu209 of BC-bPC is located 8.28 Å away from that of the corresponding residue (Glu205) in BC-eACC. In other words, it is probable that BC-bPC associates into a dimeric structure that differs from those known for BC-eACC and BC-aPC. BC-bPC elutes as a dimer upon gel-filtration chromatography (Sueda *et al.*, 2004) and the present observation is consistent with the behaviour of BC-bPC in solution. The interactions in the two types of association are summarized in Table 3: a comparison of the interactions of mol1–mol2 with those of mol1–mol3 reveals that the former are richer in salt bridges and hydrogen bonds than the latter. Accordingly, the association of mol1 and mol2 is energetically more favourable than that of mol1 and mol3 (Fig. 2 and Table 3). Hence, it may be concluded from these results that only BC-bPC forms a unique dimer structure with domain *B* contacting domains *A* and *C* of the other molecule (mol1–mol2 in Fig. 2). It should be

noted, however, that this unique dimeric structure may have occurred as a result of the division of the BC domain from the rest of the protein in bPC; native bPC is a tetrameric protein (Wood & Barden, 1977). In the structure of the divided BC domain of *Saccharomyces serevisiae* ACC, it was suggested that the protein exists as a monomer while the intact enzyme is a polymer (Shen *et al.*, 2004).

3.4. Structure of domain *B*

As the structure of BC-bPC is similar to that of BC-eACC, it is inferred that the former undergoes a conformational change similar to that of the latter upon substrate binding, *i.e.* from the open to the closed form. When the structure of BC-bPC is compared with the open and closed forms of BC-eACC (Waldrop *et al.*, 1994; Thoden *et al.*, 2000), it is noticed that domain *B* and the linkers connecting domains *B* and *C* (Val204–Glu215; loop region) exist in positions intermediate between the open and closed forms of BC-eACC (Fig. 4). In addition, the position of domain *B* relative to domains *A* and *C* in BC-bPC differs from those found in other enzymes of similar structure (Waldrop *et al.*, 1994; Kondo *et al.*, 2004). The positional change of domain *B* of BC-bPC seems to occur as a consequence of the formation of a unique dimeric structure in the crystal state (Fig. 2). From comparison with other proteins, the glycine-rich loop region in domain *B* (the Gly-loop region) of BC-bPC most resembles the corresponding region of the closed form of BC-eACC (Fig. 5).

3.5. Active-site structure

In Fig. 6, the active-site structures of BC-bPC, unliganded BC-eACC (ATP-unbound open form; Waldrop *et al.*, 1994) and liganded BC-eACC (ATP-bound closed form; Thoden *et al.*, 2000) are compared. The carbonyl O atom of Glu209 of BC-bPC at the active site points in a direction opposite to that of the corresponding residue (Glu205) of BC-eACC (Fig. 6) and it is directed outward from the ATP-binding site. In BC-eACC Glu280 exists in the vicinity of Glu205 and if the carbonyl O atom of Glu205 is oriented in the same direction as that of Glu209 of BC-bPC, the negative charges or dipoles of the carbonyl O atom and the side chain of Glu280 face each other. To mitigate such an electrostatic repulsion, the carbonyl O atom of Glu205 seems to be directed inwards, with the N atom of Asn206 directed outwards. It seems that this conformational change of Glu205 is necessary in BC-eACC for this interaction of the amide N atom of Asn206 to prevail. In BC-bPC, Ser284 corresponds to Glu280 in BC-eACC, but it is not located near Glu209. As a result, Ser284 will exert only a small effect on the orientation of the carboxylate O atom of Glu209.

The side chain of His240 of BC-bPC is also oriented differently from that of His236 in the ATP-bound closed form of BC-eACC (Fig. 6*c*), but nearly in the same direction as His236 of BC-eACC without ATP (Fig. 6*b*). Therefore, this residue undergoes a conformational change in concert with ATP binding. It is hence inferred that the side chain of this residue plays an important role in ATP binding.

As described in §1, it is conceivable that there is an acetyl-CoA-binding site on BC-bPC. Unfortunately, however, such a site could not be identified in the solved structure. Glu329–Lys334 residing between an α-helix and a β-strand may be a candidate, but does not look especially suitable for acetyl-CoA binding. The acetyl-CoA-binding site may be exposed or created in the boundary between the domains of BC dimers or tetramers when PC is associated in the native tetrameric form. Alternatively, the boundary of the BC and CT domains is another candidate. The validity of these and other possibilities awaits elucidation of the complete structure of PC.

This work was supported by a grant for the promotion of structural analysis of 3000 proteins.

References

Attwood, P. A. (1993). *Biochemistry*, **32**, 12736–12742.
Attwood, P. A. (1995). *Int. J. Biochem. Cell Biol.* **27**, 231–249.
Brünger, A. T., Adams, P. D., Clore, G. M., DeLano, W. L., Gros, P., Grosse-Kunstleve, R. W., Jiang, J.-S., Kuszewski, J., Nilges, M., Pannu, N. S., Read, R. J., Rice, L. M., Simonson, T. & Warren, G. L. (1998). *Acta Cryst.* D**54**, 905–921.
Cazzulo, J. J. & Stoppani, A. O. (1968). *Arch. Biochem. Biophys.* **127**, 563–567.
Cohen, N. D., Duc, J. A., Beegen, H. & Utter, M. F. (1979). *J. Biol. Chem.* **254**, 9262–9269.
Jitrapakdee, S. & Wallace, J. C. (1999). *Biochem. J.* **340**, 1–16.
Kissinger, C. R., Gehlhaar, D. K. & Fogel, D. B. (1999). *Acta Cryst.* D**55**, 484–491.
Kondo, S., Nakajima, Y., Sugio, S., Sueda, S., Kim, Y.-B. & Kondo, H. (2004). *Acta Cryst.* D**60**, 486–492.
Kraulis, P. J. (1991). *J. Appl. Cryst.* **24**, 946–950.
Laskowski, R. A., MacArthur, M. W., Moss, D. S. & Thornton, J. M. (1993). *J. Appl. Cryst.* **26**, 283–291.
McRee, D. E. (1993). *Practical Protein Crystallography*. New York: Academic Press.
Matthews, B. W. (1968). *J. Mol. Biol.* **33**, 491–497.
Mukhopadhyay, B., Stoddard, S. F. & Wolfe, R. S. (1998). *J. Biol. Chem.* **273**, 5155–5166.
Otwinowski, Z. & Minor, W. (1997). *Methods Enzymol.* **276**, 307–326.
Ramachandran, G. N. & Sasisekharan, V. (1968). *Adv. Protein Chem.* **23**, 283–437.
Scrutton, M. C. (1978). *FEBS Lett.* **89**, 1–9.
Shen, Y., Volrath, S. L., Weatherly, S. C., Elich, T. D. & Tong, L. (2004). *Mol. Cell*, **16**, 881–891.
Sueda, S., Islam, M. N. & Kondo, H. (2004). *Eur. J. Biochem.* **271**, 1391–1400.
Taylor, B. L., Barden, R. E. & Utter, M. F. (1972). *J. Biol. Chem.* **247**, 7383–7390.
Thoden, J. B., Blanchard, C. Z., Holden, H. M. & Waldrop, G. L. (2000). *J. Biol. Chem.* **275**, 16183–16190.
Waldrop, G. L., Rayment, I. & Holden, H. M. (1994). *Biochemistry*, **30**, 10249–56.
Wood, H. G. & Barden, R. E. (1977). *Annu. Rev. Biochem.* **46**, 385–413.